[16] Modeling Polyglutamine Pathogenesis in *C. elegans*

By HEATHER R. BRIGNULL*, JAMES F. MORLEY*, SUSANA M. GARCIA, and RICHARD I. MORIMOTO

Abstract

A growing number of human neurodegenerative diseases are associated with disruption of cellular protein folding homeostasis, leading to the appearance of misfolded proteins and deposition of protein aggregates and inclusions. Recent years have been witness to widespread development of invertebrate systems (specifically *Drosophila* and *Caenorhabditis elegans*) to model these disorders, bringing the many advantages of such systems, particularly the power of genetic analysis in a metazoan, to bear on these problems. In this chapter, we describe our studies using the nematode, *C. elegans*, as a model to study polyglutamine expansions as occur in Huntington's disease and related ataxias. Using fluorescently tagged polyglutamine repeats of different lengths, we have examined the dynamics of aggregate formation both within individual cells and over time throughout the lifetime of individual organisms, identifying aging as an important physiological determinant of aggregation and toxicity. Expanding on these observations, we demonstrate that a genetic pathway regulating longevity can alter the time course of aging-related polyglutamine-mediated phenotypes. To identify novel targets and better understand how cells sense and respond to the appearance of misfolded and aggregation-prone proteins, we use a genome-wide RNA interference-based genetic screen to identify modifiers of age-dependent polyglutamine aggregation. Throughout these studies, we used fluorescence-based, live-cell biological and biophysical methods to study the behavior of these proteins in a complex multicellular environment.

Introduction

Misfolded proteins, aggregates, and inclusion bodies are hallmarks of a range of neurodegenerative disorders including Alzheimer's disease (AD), Parkinson's disease (PD), prion disorders, amyotrophic lateral sclerosis (ALS), and polyglutamine diseases, which include Huntington's disease

* These authors contributed equally to this work.

METHODS IN ENZYMOLOGY, VOL. 412

0076-6879/06 $35.00
DOI: 10.1016/S0076-6879(06)12016-9

(HD) and related ataxias (Kakizuka, 1998; Kopito and Ron, 2000; Stefani and Dobson, 2003). Each of these disorders exhibits aging-dependent onset, selective neuronal vulnerability despite widespread expression of the related proteins, and a progressive, usually fatal, clinical course. Deposition of intracellular or extracellular protein aggregates is a well-conserved pathological feature and has been the focus of extensive investigation, as described later (Stefani and Dobson, 2003). Despite differences in the underlying genes involved, inheritance, and clinical presentation, the similarities observed have led to the idea of shared pathogenic mechanisms and the hope that insights into one process may be generalized to others.

In support of this premise is growing evidence that the cellular protein quality control system seems to be an underlying common denominator of these diseases (Dobson, 2001). For example, genes involved in protein folding and degradation, including molecular chaperones and components of the proteasome, have been shown to modulate onset, development, and progression in models of multiple neurodegenerative diseases (Bonini, 2002; Chan *et al.*, 2002; Cummings *et al.*, 1998). Furthermore, it has been suggested that despite the absence of sequence homology, different disease-related proteins share a common ability to adopt similar proteotoxic conformations (Kayed *et al.*, 2003; O'Nuallain and Wetzel, 2002) and that these might be used as therapeutic targets.

Invertebrate Models of Neurodegenerative Disease

Some of these disorders, including the polyglutamine diseases, exhibit clear familial inheritance, allowing the use of genetic studies and positional cloning to identify single gene alterations underlying the disorders (Kawaguchi *et al.*, 1994; Koide *et al.*, 1994; La Spada *et al.*, 1991; Orr *et al.*, 1993). Other diseases are more commonly sporadic, but rare familial forms have allowed the identification of candidate genes that could reveal insights into pathology. These include mutations of amyloid precursor protein in AD, parkin and α-synuclein in PD, and superoxide dismutase in ALS (Kamino *et al.*, 1992; Laing and Siddique, 1997; Lucking *et al.*, 2000; Mizuno *et al.*, 2001; Polymeropoulos *et al.*, 1997; Rosen *et al.*, 1993). Identification of these genes has led to an explosion of models to investigate the underlying pathology, identify factors and pathways that modify the disease process, and test potential therapeutic interventions.

Mouse and cell culture models continue to be mainstays to complement clinical study of these disorders for their complexity and simplicity, respectively. Recently, invertebrate models, in particular *Drosophila* and *C. elegans,* have been used to great advantage in the study of neurodegenerative disease (Driscoll and Gerstbrein, 2003; Link, 2001; Thompson and Marsh, 2003;

Westlund *et al.*, 2004). As described in more detail later for *C. elegans*, these systems represent an attractive intermediate by combining sufficient complexity to allow investigation of both cellular and behavioral phenotypes with simplicity that facilitates rapid, high-throughput testing of hypotheses.

Pathogenic mechanisms in neurodegeneration often involve a gain of function toxicity allowing these disorders to be modeled by transgenic overexpression of human disease–related proteins regardless of the presence or absence of a clear ortholog. For example, expression of polyglutamine-containing proteins is neurotoxic in both *Drosophila* retinal neurons and *C. elegans* chemosensory or mechanosensory neurons despite the absence of clear disease gene orthologs (Faber *et al.*, 1999, 2002; Parker *et al.*, 2001; Warrick *et al.*, 1998). Similar strategies have been used to examine the toxicity of APP, SOD, and α-synuclein in flies and worms (Feany and Bender, 2000; Lee *et al.*, 2005; Link, 1995, 2001; Oeda *et al.*, 2001; Shulman *et al.*, 2003; Wexler *et al.*, 2004). However, it is clear that no single model recapitulates all features of a given disease. A discrepancy common with many models is that disease-related proteins are toxic in most cell types where they have been expressed without appropriate tissue specificity. Despite the idiosyncrasies of different models, each provides unique insights that clearly validate the general approach. Presumably, features observed across disparate models, with different inherent assumptions and sources of variability, are most likely to represent key events underlying pathology.

C. elegans Models of Polyglutamine Disease

We have focused our studies largely on polyglutamine expansions as occur in Huntington's disease and related movement disorders including several spinocerebellar ataxias and Kennedy's disease (Orr, 2001; Ross, 2002; Trottier *et al.*, 1995; Zoghbi and Orr, 2000). Expression of expanded polyglutamine, with or without flanking sequences from the endogenous proteins, or when inserted into an unrelated protein, is sufficient to recapitulate pathological features of the diseases in multiple model systems (Davies *et al.*, 1997; Mangiarini *et al.*, 1996; Ordway *et al.*, 1997). This suggests that polyglutamine expansions play a central role in these disorders and supports an approach in which expression of isolated polyglutamine expansions without flanking sequences could lend insight into shared features of these disorders.

A novel feature of the polyglutamine diseases is polymorphism of the repeat length among individuals, with an apparent pathogenic threshold of 35–40 residues. Molecular genetic studies have established that Huntingtin alleles from normal chromosomes contain fewer than 30–34 CAG repeats, whereas those from affected chromosomes contain greater than 35–40

repeats (Andrew *et al.*, 1993). Analysis of patient databases has established a strong inverse correlation between repeat length and age of onset (Andrew *et al.*, 1993; Brinkman *et al.*, 1997). Similar breakpoints and length dependence are seen for the other polyglutamine repeat diseases suggesting a 35–40 residue threshold at which the disease gene products are converted to a proteotoxic state.

Here, we describe our experience using the nematode, *C. elegans*, as a model to study polyglutamine expansions. *C. elegans* is a roundworm that in its free-living form can be found in a variety of soil habitats throughout the world. In the laboratory, the animals can be readily cultured in large numbers on agar plates seeded with a lawn of *E. coli*, as wild-type adult animals reach a maximum length of approximately 1–1.5 mm. The adult stage is preceded by progression through embryonic development and four larval stages. This life cycle is completed in approximately 3 days under typical growth conditions (20–25°). Taken together with an adult lifespan of approximately 2 weeks under normal conditions, this allows experiments to be designed and carried out quite rapidly compared with other metazoan model systems.

A self-fertilizing hermaphrodite form comprises greater than 99% of *C. elegans* in normal populations, although males arise at a low frequency of ~0.01% (owing to meiotic nondisjunction) allowing construction and maintenance of genetic stocks. The hermaphrodite body plan is relatively simple, composed of only 959 somatic cells. However, this small number of cells is sufficient for the formation of multiple complex tissues types including intestine, muscle, hypodermis, and a fully differentiated nervous system. Thus, despite its simplicity and ease of handling in the laboratory, studies in *C. elegans* can offer insight into processes unique to complex multicellular organisms. In addition, the *C. elegans* system has well-established techniques for forward and reverse genetics, a wide range of mutants, and a fully sequenced genome, all of which enhance the usefulness of this model. We highly recommend two monographs published by Cold Spring Harbor Laboratory Press titled "The Nematode *C. elegans*" and "*C. elegans* II" for further information on *C. elegans*. Additional information and updates on *C. elegans* are available online as "WormBook" (http://www.wormbook.org).

In the studies described here, we have examined the fate of aggregation-prone polyglutamine proteins in a living organism and, in particular, the potential influence of physiological and genetic modifiers on these processes. For example, we wished to understand the relationship between aging and the ability of organisms to sense and respond to the appearance of misfolded and aggregation-prone proteins. In addition, we studied the expression of polyglutamine proteins in different tissue types, namely muscle cells and neurons, to better understand the effect of cell-type specific factors.

Using genome-wide RNA interference (RNAi) analysis in *C. elegans*, we sought to identify the comprehensive set of proteins or complexes that modulate the cellular protein folding environment, which we refer to as the ''protein folding buffer.'' Throughout these studies, we used powerful fluorescence-based cell biological and biophysical methods (described here in a series of detailed protocols) to examine the behavior of these proteins in a complex multicellular environment.

Visualization of Protein in a Live, Multicellular Organism

Previous studies *in vitro* had demonstrated that polyglutamine peptides exhibited nucleation-dependent aggregation kinetics proportional to repeat length (Chen *et al.*, 2001; Scherzinger *et al.*, 1997), reminiscent of the inverse correlation between polyglutamine length and age-at-onset observed in the human diseases (Chen *et al.*, 2002). However, studies on polyglutamine-mediated toxicity in animal models had examined only the extreme ends of the spectrum comparing the effects of very short (<30Q) or very long (>60Q) repeats. We chose to examine the distinctive properties of polyglutamine proteins at the apparent pathogenic threshold (Q30–Q40) in the crowded macromolecular environment of the cell.

We generated a series of transgenic animals expressing polyglutamine repeats of different lengths in body-wall muscle cells, with greater resolution near the apparent threshold (Q0, Q19, Q29, Q33, Q35, Q40, Q44, Q64, and Q82) fused to YFP. In young adult animals (3–4 days old), we found a clear length-dependent shift in the subcellular localization of the proteins, because repeat lengths of Q35 or less were localized diffusely as soluble proteins (Fig. 1A), but repeat lengths of Q40 and greater were localized in aggregates (Fig. 1A).

To determine whether the properties of polyglutamine proteins observed in muscle cells were tissue specific, we expressed a range of polyglutamine proteins in the nervous system of *C. elegans*. Polyglutamine proteins in *C. elegans* neurons displayed Q-length–dependent changes in protein localization similar to that observed in muscle cells. Expression of YFP alone or YFP fused to Q19, Q35, or Q40 resulted in a soluble distribution pattern (Fig. 1B). The distribution of Q67::YFP or Q86::YFP in the nervous system was distinctly different from smaller glutamine tracts, with the protein localized to discreet foci (Fig. 1B). Although the trend of length-dependent changes in the localization of polyglutamine proteins is consistent between muscle and neurons in *C. elegans*, the aggregation threshold seems to be lower in muscle cells at this level of resolution. The use of additional assays described here, including Fluorescence Recovery After Photobleaching (FRAP), reveals that Q40 is also the threshold for changes

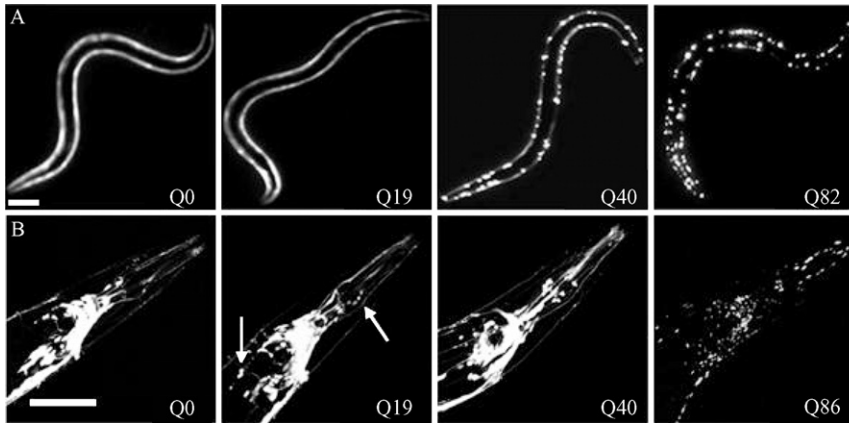

FIG. 1. Length-dependent aggregation of polyglutamine::YFP fusion proteins in *C. elegans*. (A) Fluorescent images of 3–4-day-old *C. elegans* expressing different lengths of polyglutamine::YFP in body-wall muscle cells. Bar = 0.1 mm. (B) Fluorescent images of *C. elegans* expressing different lengths of polyglutamine::YFP throughout the nervous system of 4-day-old animals. Images are flattened, confocal z-stacks of *C. elegans* head, scale bar = 50 μm. Neuronal cell bodies are significantly smaller than body-wall muscle cells and foci, such as those indicated by the arrows in Q19 (B) are cell bodies. In both tissue types, expressing YFP or Q19::YFP results in diffuse fluorescence in all expressing cells, whereas animals expressing >80 glutamine repeats exhibited distribution into fluorescent foci. Animals expressing Q40::YFP in muscle cells showed a polymorphic phenotype with both diffuse and punctate fluorescence distribution (A), whereas no changes in Q40::YFP distribution are visible in the neuronal model at this level of microscopic resolution (B).

in the properties of polyglutamine proteins in neurons as well as in muscles. Together, these models establish a system allowing the simultaneous visualization of aggregation and toxicity in multiple tissue types in a single organism, allowing further studies to identify physiological and genetic modifiers.

Generating Transgenic C. elegans*–Expressing Polyglutamine Proteins*

Plasmid Construction. Construction of polyglutamine vectors for expression in muscle cells was as described previously (Morley *et al.*, 2002). Pan-neuronal polyglutamine expression was achieved by cloning 3.5 kb of DNA upstream of the *C. elegans* gene, F25B3.3, along with the first five codons with a point mutation of the start codon to ATC (gift of Dr. David Pilgrim). This fragment was cloned into pPD95.79 (gift of Dr. Andrew Fire) between the *Pst1* and *BamH1* sites generating $P_{F25B3.3}$. Glutamine tracts were established by sequencing and inserted into a second vector containing CFP (pECFP-N1, Clonetech) between the *KpnI* and *BamH1*

sites. Polyglutamine::CFP fragments were generated by addition of a 3′ *Bsm1* site following Q(n)CFP in pECFP-N1 by PCR amplification. The resulting Q(n)CFP fragments and $P_{F25B3.3}$ were digested with *Kpn1/Bsm1* and ligated. Constructs containing polyglutamine expansions labeled with YFP were generated by removing CFP from $P_{F25B3.3}$Q(n)::CFP and inserting YFP from pEYFP-N1 (Clonetech) between *Age1* and *Not1* sites.

Generation of Transgenic Strains. Nematodes were raised and handled using standard methods unless otherwise noted (Brenner, 1974). Generation of transgenic animals expressing polyglutamine proteins in muscle cells was as described previously (Morley *et al.*, 2002). For generation of transgenic animals expressing pan-neuronal polyglutamine, DNA encoding $P_{F25B3.3}$Q(0, 19, 29, 40, 67, 86)::CFP or YFP was injected into wild-type animals (N2) at 50 ng/μl. Of note, in *C. elegans*, heritable transgenes result from the assembly of injected DNAs into large extrachromosomal arrays (Mello *et al.*, 1991). Depending on copy number and other factors, expression of the gene of interest may vary somewhat in independent lines; therefore, it is important to isolate and analyze multiple lines for a given transgene to ensure homogeneity of phenotype. This is also important to ensure that any phenotypes are not the result solely of transgene expression levels, although we suggest using a biochemical approach, such as Western blots, to compare protein expression levels between transgenic lines. Finally, it is of critical importance that transgenic lines are frozen as soon as possible after they have been generated. We have observed that animals kept in continuous culture, especially those expressing large, toxic glutamine tracts, eventually adapt to the transgene. This has been more evident in various behavioral assays used to establish toxicity rather than aggregation. The time required for animals to adapt varies widely depending on the transgene and various stressors, so we cannot recommend how long lines should be kept in culture. However, we do suggest thawing lines before any new or critical assay.

The Use of Fluorescence Imaging in C. elegans

High-Resolution Imaging in C. elegans. Animals used for live imaging are mounted on a glass slide with a pad of 3% agarose. The agarose pad provides a ''cushion'' for the animals to sink into when the coverslip is added and prevents them from being crushed, allowing individual animals to be repeatedly imaged over time. Animals are immobilized by 1 m*M* levamisole, an acetylcholine agonist that causes permanent contraction of muscle cells. It is important to note that although levamisole paralyzes the body-wall muscle cells of *C. elegans*, animals should continue to display erratic pharyngeal pumping, indicating that they have survived the mounting process.

Imaging and fluorescence-based biophysical experiments presented here were performed on a Zeiss LSM, 510 Meta confocal microscope. For *C. elegans*, a 63× water objective with a 1.4 numerical aperture was used. Because animals are mounted in agarose, a water objective is preferable to an oil immersion objective. For optimal imaging, animals should be well spaced on the slide and the coverslip carefully sealed to prevent the agarose pad from drying out and desiccating the animal during imaging.

Aggregate Quantification. Animals expressing polyglutamine aggregates in muscle cells were viewed at 100× magnification using a stereomicroscope equipped for fluorescence, and the number of polyglutamine aggregates was counted. Aggregates were defined as discrete structures with boundaries distinguishable from surrounding fluorescence on all sides. Aggregate size in muscle cells, when measured using confocal microscopy, typically ranged from 1 × 5 μm. At 100× magnification, we were able to detect >80% of aggregates observable at higher magnifications. Repeated aggregate counts by the same observer and independent observers in blinded analyses varied by less than 10%. Polyglutamine aggregate size varies depending on tissue type, and aggregates in neurons were smaller (typically less than 2 μm in diameter), because their growth is limited by the small size of neurons relative to body-wall muscle cells.

Biophysical Analysis of Polyglutamine Proteins in C. elegans

A clear advantage provided by this system was our ability to readily visualize aggregates in an intact organism. This allowed us to apply fluorescence-based cell biological techniques to examine the properties of polyglutamine proteins in the living animal. For example, we used Fluorescence Recovery After Photobleaching (FRAP) to determine whether the shift in polyglutmine::YFP cellular distribution corresponded to a transition of these proteins from a soluble to an aggregated state. FRAP and other biophysical techniques can be adapted for *C. elegans* with very few changes to the processes established for studying cultured cells.

Fluorescence Recovery After Photobleaching. One of the most critical requirements for FRAP is a good sample; in this case a well-mounted animal exhibits minimal movement and provides access to the appropriate cells. The process of mounting *C. elegans* for microscopy was described previously; however it is often difficult to find animals that are sufficiently still and in the correct orientation. Therefore, we recommend preparing at least two slides with ~5–10 animals mounted on each slide. To minimize movement, animals should not be mounted immediately before FRAP experiments. We typically allow at least 30 min before experiments for maximal effectiveness of levamisole treatment.

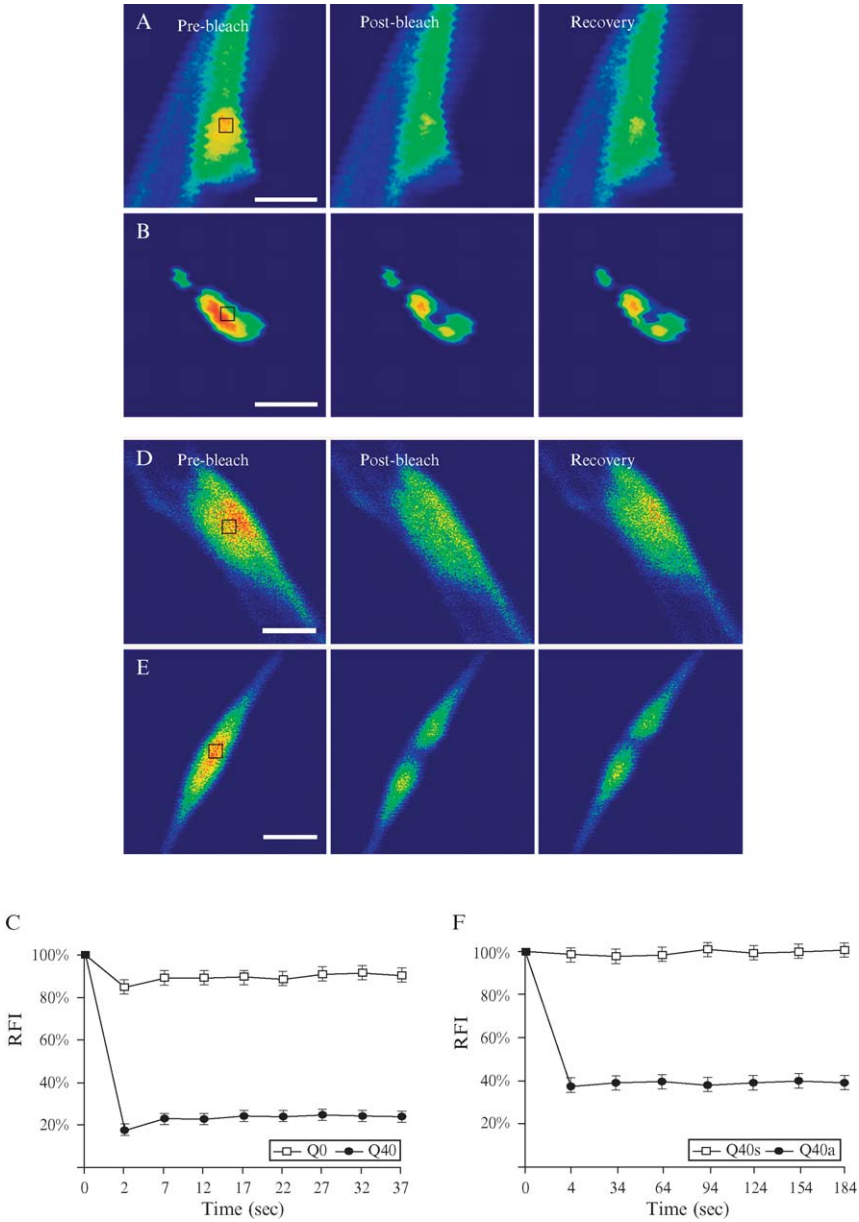

FIG. 2. FRAP analysis of polyglutamine::YFP solubility in living animals. FRAP distinguishes between Q0::YFP (A) and a Q40::YFP foci (B) in muscle cells. Images presented are representative and include an image before photobleaching (pre-bleach) of the boxed area (black box), immediately after photobleaching (post-bleach) and after a recovery period (time

The data presented here were generated by FRAP analysis on animals expressing various lengths of polyglutamine proteins fused to a C-terminal YFP. Therefore, both imaging and photobleaching used a laser with a wavelength of 514 nm, specific for YFP. Excitation for imaging purposes was performed at 0.1% laser power transmission. This low percentage of transmission was selected for imaging to minimize photobleaching while still providing sufficient image quality for data analysis. Photobleaching used 100% transmission of the 514 nm laser over a region of interest (ROI) with iterations sufficient to photobleach the sample. The size of the ROI, number of photobleaching iterations and the imaging transmission should be adjusted on the basis of the specific properties of the sample. For example, *C. elegans* muscle cells are much larger than neurons, and, consequently, polyglutamine aggregates become larger in muscle cells than in neurons, as indicated previously. Therefore, in muscle cells, the ROI was fixed at an area of 3.6 μm^2 (25 $\times$ 25 pixels), whereas in neurons, the ROI was 10 $\times$ 10 pixels. Once these parameters are determined, they must remain consistent between experiments for data analysis.

Images for analysis should be collected before and after photobleaching. The duration of the recovery period is dependent on the protein of interest but should continue until fluorescent recovery has plateaued. In the data presented in Fig. 2, the ROI was bleached for 4 sec (five iterations at 100% laser power), after which an image was collected every 30 sec for up to 5 min.

FRAP Data Analysis. Relative fluorescence intensity (RFI) was determined using the equation: $RFI = (T_t/C_t)/(T_0/C_0)$. T_0 indicates the intensity of fluorescence in the ''test'' ROI before photobleaching, and T_t is intensity in the same area at a given time after bleaching. Data should be normalized against an unbleached area in the same cell as a control for photobleaching and autofluorescence. Therefore, C_0 is the fluorescence intensity of a control area before bleaching and C_t the same area at a given time after bleaching (Phair and Misteli, 2000). In choosing the control area, it is better to pick an area within the same cell being bleached. This is especially important for

indicated in accompanying graph). As expected, Q0 recovers rapidly from photobleaching (A), whereas Q40 protein in foci does not recover from photobleaching (B), consistent with an insoluble protein. Bar = 2 μm. (C) Results from FRAP are quantified by determining the relative fluorescence intensity (RFI) for each time point the graph represents the average of analysis of a minimum of five independent measurements. Error bars indicate SEM. In neurons, FRAP was able to distinguish between a soluble (40s, D) and insoluble species (40a, E) of the same Q40::YFP protein, quantified in (F). Scale bars indicate 2 μm. Quantification of neuronal data is the mean of five neurons for 40s and 10 neurons for 40a. Error bars indicate SEM.

FRAP experiments in *C. elegans,* because even when anesthetized, animals may move unexpectedly, changing the intensity in the ROI without affecting the background or other cells. Any movement of the cell of interest will skew data automatically generated by the ROI function in the AIM software associated with a Zeiss LSM confocal microscope. The intensity data generated by the ROI function quantifies intensity in the same location for each time point so if there is any movement, results will only be accurate until that point. Therefore, when intensity of an ROI is being determined, each time frame *must* be examined individually for any shift in the ROI. This is a significant difference from FRAP analysis in cells that remain quite still by comparison. Data resulting from analysis using the preceding equation will generate an RFI for every time point at which an image is collected and is used to generate the graphs shown in Fig. 2.

FRAP Analysis of Polyglutamine Proteins in a Multicellular Organism. We used FRAP to determine whether the shift in polyglutmine::YFP cellular distribution corresponded to a transition of these proteins from a soluble to an aggregated state. Furthermore, FRAP can be performed on individual cells in a live animal; significant advantages to traditional biochemical approaches to identifying aggregates. We reasoned that soluble YFP-tagged proteins in the cytoplasm would diffuse freely and recover rapidly after photobleaching. In contrast, fluorescent proteins with limited mobility within an aggregate should exhibit little or very slow recovery after photobleaching. Photobleaching of diffuse Q0::YFP from young animals led to an immediate 100% fluorescence recovery (Fig. 2A, C), consistent with the biophysical properties of soluble proteins; this result has also been demonstrated biochemically by SDS-PAGE and immunoblotting of bulk samples (Nollen *et al.*, 2004; Satyal *et al.*, 2000). In contrast, the fluorescent signal associated with foci in muscle cells of Q40 animals does not recover after photobleaching consistent with restriction within aggregates (Fig. 2B, C). These results are consistent with the polyglutamine length-dependent changes in localization observed visually and provide a quantitative measure of solubility that can be used to define aggregation in *C. elegans*.

When FRAP is applied to polyglutamine proteins in *C. elegans* neurons, a similar trend is observed: as the length of glutamine tracts increases, protein solubility decreases. However, FRAP experiments on multiple neurons distributed throughout a single animal revealed that Q40::YFP recovery from photobleaching varies widely. Q40 protein solubility ranges from rapid (Fig. 3D, F), similar to that observed for soluble Q19, to completely immobile Q40::YFP (Fig 3E, F), similar to the Q86 aggregates despite the absence of overt visual foci in Q40 animals. The small size and complex structures of neurons in *C. elegans* prevented visual detection of

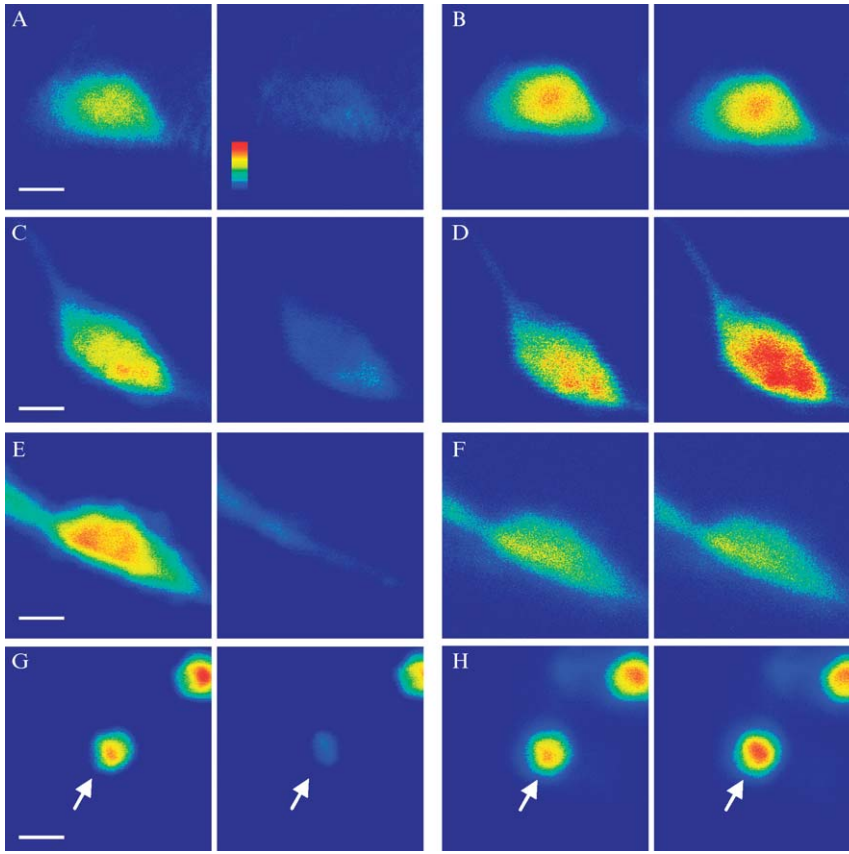

FIG. 3. Expanded polyglutamine proteins FRET *in vivo*. Q86 protein in neuronal aggregates exhibits FRET, indicating close and roughly ordered interactions at the molecular level. YFP photobleaching is seen on the YFP channel (A, C, E, and G) and its effect on the CFP donor in the same cell (B, D, F, H). CFP and YFP coexpression (A, B) do not FRET, $E^c = 0.08$ ($\pm$ standard deviation of 0.16), $n = 5$. Animals expressing CFP::YFP do FRET (C, D), $E^c = 0.25$ ($\pm$ 0.08), $n = 20$. Neurons coexpressing Q19::CFP and Q19::YFP (E, F) do not FRET, $E^c = -0.08$ ($\pm$ 0.05), $n = 15$, whereas coexpression of Q86::CFP and Q86::YFP (G, H) does produce FRET, $E^c = 0.22$ ($\pm$ 0.08), $n = 17$. Cells shown are representative of FRET experiments. Intensity is by a color scale (G), where blue is least intense and red is most intense. Scale bar = 2 μm.

changes in protein solubility at low magnification, as were observed in muscle cells. These data provide an example of the usefulness of FRAP as a technique for establishing subtle changes in protein solubility in specific cells of a live, metazoan model.

Fluorescence Resonance Energy Transfer (FRET). FRET is a technique developed principally for *in vitro* biochemical studies and applied to cell culture to address *in vivo* questions of macromolecular interactions. The resolution of this technique is in the nanometer range; FRET is maximal at 50 Å and will not occur if proteins are more than 100 Å apart when using CFP and YFP fluorophores. The second condition required for FRET is that proteins are appropriately oriented to enable dipole–dipole interactions between fluorophores; proteins must be roughly parallel for energy transfer between fluorophores (Miyawaki, 2003; Miyawaki and Tsien, 2000). This technique has been widely used to show protein interactions *in vitro* and in cell culture (Kim *et al.*, 2002; Tsien, 1998), and we were interested in establishing whether FRET could be performed in *C. elegans* to determine whether polyglutamine proteins are sufficiently ordered and in molecular proximity for energy transfer to occur between CFP (donor) and YFP (acceptor).

FRET experiments in *C. elegans* were performed by an indirect method; combined donor and acceptor photobleaching (Berney and Danuser, 2003; Wouters *et al.*, 1998). When fluorophores are in sufficient proximity and the appropriate orientation, energy is transferred from the donor to the acceptor. This results in decreased donor intensity and increased acceptor intensity. In conditions where FRET is occurring, photobleaching of the acceptor blocks energy transfer causing donor intensity to increase. Thus, measuring donor intensity before and after acceptor photobleaching is an indirect measurement of FRET, whereas determining acceptor emission in the presence or absence of donor excitation would be a direct measure of FRET.

We chose to measure FRET indirectly, using the acceptor photobleaching technique, to minimize the potential for excitation bleed-through. YFP is also excited by the 458 nm laser used to excite CFP in *C. elegans*. Therefore, we measured FRET indirectly by quantifying CFP emission before and after YFP photobleaching and only needed to control for emission bleed-through. There are two approaches to controlling emission bleed-through. First is careful selection of emission filters that do not allow any overlapping emissions, although this may result in some loss of signal intensity. The data presented here used this approach, and the setup included an HFT 458/514 primary dichroic beam splitter, a 480–520 nm bandpass filter on the CFP detection channel, and a bandpass filter from 524–546 on the YFP detection channel.

The second option for setting up the microscope to minimize bleed-through is to capture both donor and acceptor emission simultaneously using a filter such as the Zeiss ''Meta Detector.'' This detector, when used in the ''Lambda Scan Mode'' will scan across all emission wavelengths and

bin all emissions into 10.7 nm wavelengths. The resulting spectra can be unmixed using the linear unmixing algorithm to maximize the available signal while minimizing spectral overlap.

For imaging, excitation of CFP and YFP was at 5% transmission of 458 nm laser line. YFP photobleaching was done with 514 nm laser at 100% transmission. To photobleach YFP in neurons of *C. elegans*, an ROI of 25 × 25 pixels was bleached for 50 iterations (~10 sec) while using a 63× water objective, numerical aperture 1.4, at 9× scan zoom. Conditions were optimized to photobleach YFP throughout the entire *C. elegans*' neuron so the ROI selected was larger than that used in FRAP (10 × 10) in which only a portion of each neuron was photobleached. Both the duration and area of photobleaching should be adjusted for the sample, cell, and fluorophore of interest. Images should be obtained before and after photobleaching.

FRET Data Analysis. Normally, FRET data are presented as ratio images to provide a visual representation in the change in donor intensity after acceptor photobleaching. However, even immobilized *C. elegans* twist slightly during imaging causing three-dimensional misalignment of sequential images that hinders alignments for ratio images. Therefore, representative images from FRET experiments display individual images before and after YFP bleaching for both acceptor and donor intensity (Fig. 3). Calculation of E^c included a control area, outside of the photobleached region, to correct for any movement of the animal. Because the entire cell of interest is photobleached, the control was an adjacent cell.

There are several methods to determine molecular interactions indicated by FRET, and these are reviewed extensively in Berney and Danuser (2003). Of particular interest is their observation that when using the acceptor photobleaching technique, incomplete photobleaching increases the error in calculations of FRET efficiency. Therefore, we excluded from analysis cells with more than 10% acceptor fluorescence intensity remaining after photobleaching to minimize error. Calculating the FRET coefficient provides an indication of how efficient FRET is in the sample of interest. We calculated the FRET coefficient using the equation $(E^c) = 1 - (C_{ab}/C)(T/T_{ab})$ where *ab* = after bleaching, *C* = unbleached control cell, *T* = experimental cell, where YFP is bleached (Berney and Danuser, 2003).

FRET Reveals Intermolecular Interactions of Polyglutamine Proteins in a Multicellular Organism. To establish whether FRET could be observed in single cells of a live animal, we generated as a positive control *C. elegans* expressing a CFP::YFP chimera with a flexible linker separating the two fluorophores (Kim *et al.*, 2002). FRET experiments performed on the neuronal CFP::YFP positive control by photobleaching the YFP acceptor (Fig. 3C) resulted in increased donor (CFP) intensity as expected, $E^c = 0.25$

(± 0.08) (Fig. 3D). As a negative control, animals coexpressing CFP and YFP from separate constructs were tested. After YFP photobleaching (Fig. 3A), there was no visible increase in CFP intensity (Fig. 3B) demonstrating, as expected, that FRET was not occurring, $E^c = 0.08$ (± 0.16). With FRET efficiencies from control animals as reference points, *C. elegans* expressing both Q19::CFP and Q19::YFP were tested. Q19::YFP photobleaching (Fig. 3E) had no visible effect on CFP intensity, $E^c = -0.08$ (± 0.05) (Fig. 3F), similar to negative control animals (Fig. 3B). In contrast, animals coexpressing Q86::CFP and Q86::YFP showed an increase in CFP intensity (Fig. 3H) after YFP photobleaching, $E^c = 0.22$ (± 0.08), (Fig. 3G). FRET positive aggregates were detected in a wide range of neurons and visible redistribution of Q86 into foci, combined with SDS resistance, FRAP, and FRET data, shows that large polyglutamine expansions form insoluble, ordered aggregates in neurons throughout the nervous system of *C. elegans*.

Combining Visualization of Polyglutamine Proteins with other C. elegans *Techniques*

Behavioral Assays Determine Polyglutamine-Mediated Cellular Dysfunction. Motility in *C. elegans* can be assayed as described in Morley *et al.* (2002). Individual animals at the indicated ages were picked to fresh plates and their tracks recorded (Fig. 4A) at indicated time intervals using a CCD camera and Leica dissection stereomicroscope (8× magnification), and distance traveled was determined using a ruler calibration macro in the Openlab software program (Improvision). Dividing this distance by the time interval gave the motility index for each animal. Statistical significance of the results was determined by a chi-squared test. Because the polyglutamine transgenes were carried on extrachromosomal arrays, some animals in the population were nontransgenic and consequently provided internal controls. Motility values for wild-type (N2) and nontransgenic control groups were indistinguishable from one another.

Young adult animals expressing polyglutamine expansions of ≤35 exhibited motility similar to wild type (Fig. 4B). In contrast, we observed a ~10-fold reduction in motility of young adult Q82 animals (Fig. 4B). Q40 animals, which had aggregates in some cells but not in others, exhibited an intermediate motility defect with a high degree of variation in the intensity of loss of motility across a population (Fig. 4B) that corresponded directly with the degree of aggregate formation in any given animal (Morley *et al.*, 2002).

Aging Influences the Threshold for Polyglutamine Aggregation and Toxicity. Although aggregation-prone proteins are expressed throughout the lifetime of patients, pathology associated with diseases such as

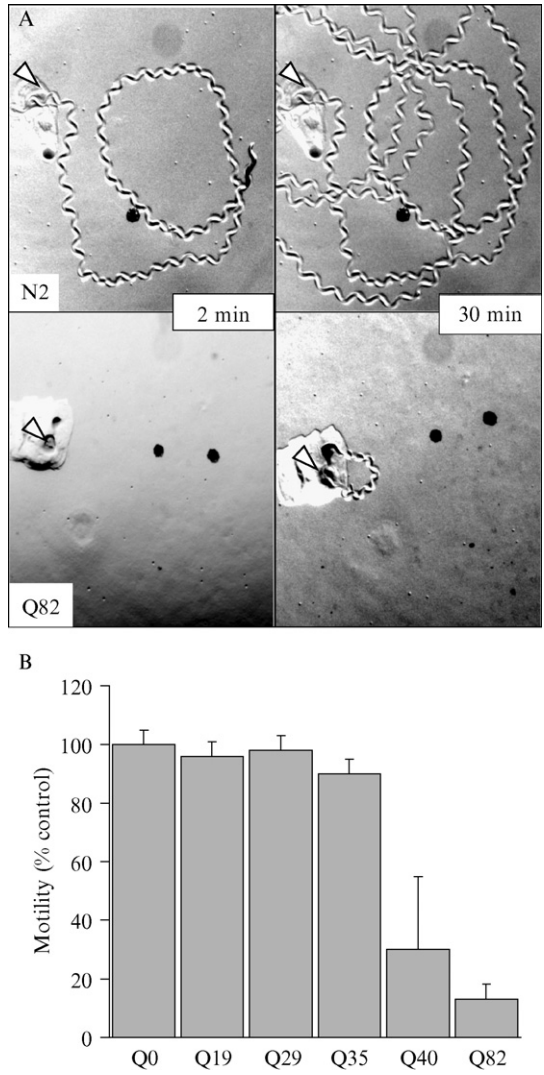

FIG. 4. Behavioral analysis of polyglutamine-mediated cellular dysfunction. (A) Time-lapse micrographs show tracks left by 5-day-old wild type (N2) and Q82 animals 2 and 30 min after being placed at the position marked by the arrowhead. (B) Quantification of motility index for 4- to 5-day-old Q0, Q19, Q29, Q35, Q40, and Q82 animals reveal polyglutamine length-dependent toxicity. Data are mean ± SD for at least 50 animals of each type as percentage of N2 motility. (Morley *et al.*, 2002. Copyright 2002, National Academy of Sciences, U.S.A.)

Huntington's, Alzheimer's, and Parkinson's are typically not manifest until middle or old age. This motivated us to study the behavior of polyglutamine proteins during aging. Indeed, a major advantage of the *C. elegans* system was our ability to follow the behavior of fluorescent polyglutamine proteins in individual animals over their entire lifetimes. We found that the threshold for aggregate formation described previously for young animals was dynamic as the animals aged. At 3 days of age or less, only animals expressing Q40 or greater exhibit aggregates (Fig. 5A). However, at 4–5 days of age, the threshold shifts as aggregates appear in Q33 and Q35 animals (Fig. 5A). The threshold again shifts to Q29 with appearance of aggregates in aged animals (>9–10 days) (Fig. 5A). In all cases, we observed a coordinated age-dependent loss of motility relative to controls that paralleled the accumulation of polyglutamine aggregates (Fig. 5B). Thus, the threshold for polyglutamine aggregation and toxicity is not static or strictly repeat length-dependent, likely reflecting a balance of different factors including repeat length and changes in the cellular protein folding environment over time.

On the basis of these results, we wondered whether this behavior resulted from the intrinsic properties of a protein motif, or whether changes over time reflect the influence of aging-related alterations in the cellular physiology. The idea that the molecular determinants of longevity might influence polyglutamine-mediated toxicity is supported by observations that the time until polyglutamine-mediated pathology develops—days in *C. elegans*, weeks in *Drosophila*, months in mice, and years in humans—correlates approximately with the lifespan of the organism. Here, again, the *C. elegans* model was a tremendous advantage, because the availability of mutants with extended lifespans allowed us to test these ideas directly.

To accomplish this, we generated transgenic animals expressing Q82::YFP in the background of animals with extended longevity. In *C. elegans*, *age-1* encodes a phosphoinositide-3 kinase that functions in an insulin-like signaling pathway (ILS), and mutations in this gene can extend lifespan by 1.5–2 fold (Guarente and Kenyon, 2000; Morris *et al.*, 1996). When expressed in long-lived animals, both aggregation (Fig. 5C) and toxicity (Fig. 5D) of polyglutamine proteins were substantially delayed (Morley *et al.*, 2002). Furthermore, the suppression of polyglutamine aggregation and toxicity was entirely dependent on the activity of *daf-16*, a forkhead transcription factor that functions downstream of *age-1* in the ILS pathway and is required for extended lifespan (Guarente and Kenyon, 2000; Lin *et al.*, 1997; Ogg *et al.*, 1997). Thus, the dual effects of *age-1* on longevity and polyglutamine-mediated toxicity share a common genetic pathway.

Genome-Wide RNAi Screening Defines Novel Regulators of Polyglutamine Aggregation and Toxicity. The dynamic threshold for polyglutamine

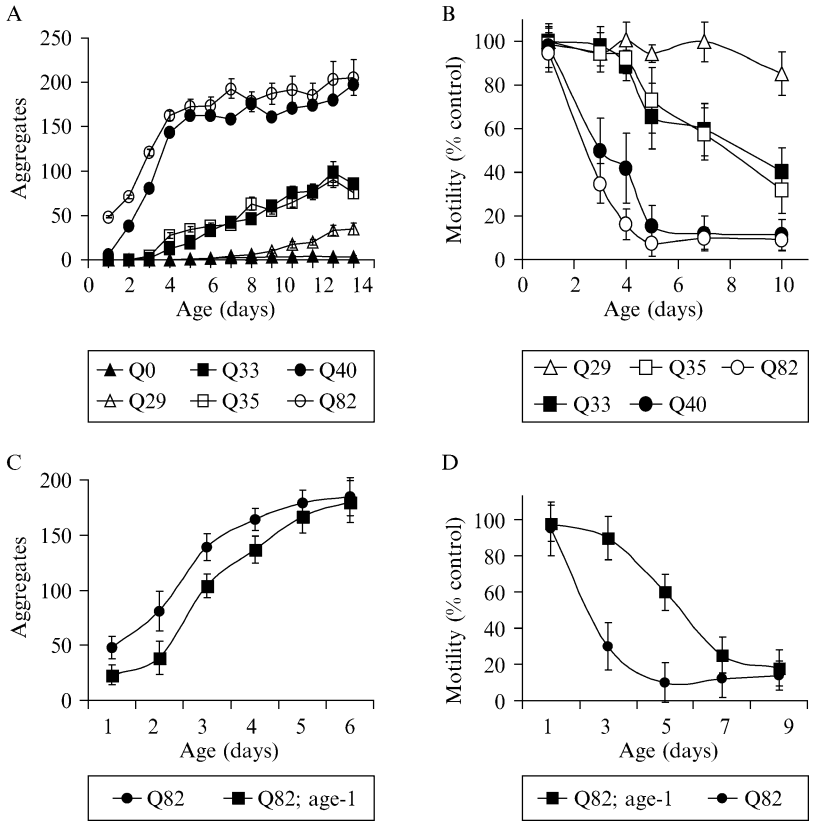

FIG. 5. Influence of aging on polyglutamine aggregation and toxicity. (A) Repeat length-dependent accumulation of polyglutamine aggregates during aging. Data are mean ± SEM. Twenty-four animals of each type are represented at day 1. Cohort sizes decreased as animals died during the experiment, but each data point represents at least five animals. (B) Motility index as a function of age for the same cohorts of animals described in A. Data are mean ± SD as a percentage of age-matched Q0 animals. Mutations in the *C. elegans* gene, *age-1* extend lifespan and alter polyglutamine pathogenesis. (C) When polyglutamine expressing animals are crossed into an *age-1* background we observe that extending lifespan in *C. elegans* delays the onset of aggregation. Data are mean ±SEM. (D) Increased lifespan also delays the onset of polyglutamine-mediated toxicity as measured by motility. Data are mean ± SD for 30 animals of each type. Motility of nontransgenic wild-type and *age-1* animals was similar to that of wildtype (N2). (Morley *et al.*, 2002. Copyright 2002, National Academy of Sciences, U.S.A.).

aggregation and toxicity demonstrates that the fate of these proteins is not an all-or-none outcome solely on the basis of repeat length and implies the presence of a cellular buffering system to prevent proteotoxicity. Thus, this model provided a substrate to which we could apply the power

of *C. elegans* forward and reverse genetics to define components of the cellular buffer and uncover novel modifiers of polyglutamine-induced pathology.

The results previously described identify ILS as a genetic pathway that can influence the course of polyglutamine-mediated phenotypes. What other pathways might exert similar effects? Numerous overexpression and genetic studies in mammalian (Cummings *et al.*, 2001) and *Drosophila* (Fernandez-Funez *et al.*, 2000; Warrick *et al.*, 1999) models have identified various enhancers or suppressors of polyglutamine-mediated aggregation and toxicity. This is well-illustrated by the large number of approaches in which various molecular chaperones either alone or in combination have been shown to influence polyglutamine-mediated phenotypes (Bonini, 2002; Carmichael *et al.*, 2000; Chai *et al.*, 1999; Cummings *et al.*, 1998, 2001; Warrick *et al.*, 1999). Although one could argue which of these modifiers is the "key" to determining the fate of aggregation-prone proteins, we interpret these results to suggest that the transition of polyglutamine proteins from a soluble to an aggregated state is the result of a delicate balance in which multiple pathways are involved. To identify the complete protein-folding buffer involved in polyglutamine transition from a soluble to an aggregated state, we used a genome-wide RNAi approach.

RNAi is a commonly used reverse-genetics approach in *C. elegans* (Fire *et al.*, 1998; Wang and Barr, 2005) allowing the targeted down-regulation of specific genes by introduction of small fragments of cognate double-stranded RNAs. Although initially used to test the function of single or small groups of candidate genes, this technique has been adapted to genome-wide screens with the Ahringer laboratory's construction of a library consisting of 16,757 bacterial clones covering 86% of the predicted *C. elegans* genome (Fraser *et al.*, 2000; Kamath *et al.*, 2003). RNAi has the additional advantages of allowing the detection of lethal positives and the immediate identification of the target genes. However, genome-wide RNAi screens may miss certain genes because of variation in mRNA depletion or relative inefficiency of RNAi in specific tissues, of which neurons are an example. Nevertheless, this approach offers an extremely powerful and rapid tool to identify the set of genes that modify a given phenotype.

To identify genes that prevent polyglutamine aggregate formation we used *C. elegans* strains expressing polyglutamine lengths close to the aggregation threshold, Q33 and Q35 strains, in an RNAi genetic screen.

Genome-wide RNAi Screening in C. elegans. The full-genome RNAi screen was performed in a 96-well format by feeding RNAi bacteria to animals in liquid culture. Construction of the RNAi library used in the genetic screen was described originally by Ahringer's group, and our initial use was described in Nollen *et al.* (Ashrafi *et al.*, 2003; Fraser *et al.*, 2000;

Nollen *et al.*, 2004). The RNAi library used is now commercially available thru ''MRC geneservice'' at http://www.hgmp.mrc.ac.uk/geneservice/index.shtml.

Animals were synchronized by NaOCl bleaching and overnight hatching in M9. In each well, 10–15 L1 larval-stage animals were suspended in 50 μl of M9 plus (M9, 10 μg/ml cholesterol, 50 μg/ml ampicillin, 12 μg/ml tetracycline, 200 μg/ml isopropyl β-D-thiogalactoside [IPTG] and 0.1 μg/ml fungizone) and added to 80 μl of an overnight culture of RNAi bacteria induced by IPTG for 4 h. The animals were grown at 23° with continuous shaking at 150 rpm (New Brunswick Scientific Incubation shaker). Q35 animals were scored for foci formation by visual inspection after 72 h. RNAi-producing bacteria that induced more than five visible foci in >30% of the animals in a well were scored as aggregation enhancers. All positive RNAi clones were confirmed in an independent experiment and scored for aggregate formation in Q0, Q24, and Q33 animals. A gene was scored as a positive when it induced early onset of aggregation in both Q33- and Q35-expressing animals but not in Q0 and Q24 animals. This criteria ensured that the genes identified where polyglutamine expansion specific. The gene targets of the positive RNAi clones were verified by sequencing of the insert of the RNAi plasmids.

A total of 186 modifiers were identified, comprising five major classes: genes involved in RNA metabolism, protein synthesis, protein folding, protein trafficking, and protein degradation (Nollen *et al.*, 2004). Examples of some of these genes are RNA helicases, splicing factors, and transcription factors for RNA metabolism; initiation and elongation factors and ribosomal subunits for protein synthesis; chaperonins and Hsp70 family members for protein folding; nuclear import and cytoskeletal genes for protein trafficking; and proteasomal genes for protein degradation. Although numerous distinct biochemical activities are represented by the different modifiers, a common feature is an expected imbalance between protein synthesis, folding, and degradation triggered by their disruption. In this context, these five classes can then be further grouped in two major categories: genes whose disruption leads to an increase in misfolded protein production and genes that when disrupted lead to a decreased clearance of misfolded proteins and proper protein turnover. Together, these results reveal that the transition between soluble and aggregated states of polyglutamine proteins is regulated by a much more complex integration of events, extending beyond the immediate involvement of chaperone-mediated folding and proteasomal degradation. In addition these findings validate an approach allowing our group and others to screen RNAi libraries against model systems for multiple neurodegenerative diseases to identify similarities and differences in the set of modifiers observed to better understand the conserved or unique aspects of their pathophysiology.

Discussion

C. elegans *Models of Polyglutamine-Mediated Toxicity and Aggregation*

We describe here two *C. elegans* models expressing isolated polyglutamine repeats in neurons or in muscle cells to investigate not only the pathogenesis of HD and related disorders but also to uncover the genes and associated pathways that regulate the protein folding environment. Our model differs from the human diseases in that we expressed isolated polyglutamine motifs rather than those in the context of disease-related proteins. Although protein context and posttranslational modifications of flanking sequences are increasingly recognized to play a role in pathology (Chai *et al.*, 2001; Chen *et al.*, 2003), we reasoned that studying isolated polyglutamine expansions would lend insight into the conserved features underlying the different pathologies. In support of this idea, our genome wide RNAi screen identified multiple molecular chaperones that have been implicated in polyglutamine diseases, AD and PD. Furthermore, expression of isolated polyglutamine tracts in both neurons and body-wall muscle cells of *C. elegans* recapitulated numerous features of the human diseases, including polyglutamine length-dependent aggregation and toxicity. More subtle features were also observed, specifically variability in aggregate formation and severity of motility defect observed in Q40 animals (Figs. 1 and 4). These observations relied on unique characteristics of *C. elegans*, in particular its' transparency, which enabled us to apply fluorescence-based biophysical assays such as FRAP and FRET to a live, multicellular animal. These studies represent the initial stages of applying biophysical approaches to *C. elegans,* and future studies may extend the use of these techniques to generate more precise, quantitative data on the polyglutamine proteins *in vivo*. These might include examining the relative proportions of soluble versus insoluble polyglutamine protein in specific cells or determining how solubility and/or intermolecular interactions of polyglutamine proteins compare with other aggregation prone proteins.

Using C. elegans *to Identify Modifiers of Polyglutamine Pathogenesis*

Another important characteristic of *C. elegans* in our studies was the animals' short lifespan and the availability of genetic mutants effecting lifespan. The ability to combine visualization of polyglutamine aggregates in live animals with mutations conferring longevity enabled us to demonstrate that increasing lifespan delays polyglutamine aggregation and toxicity. These results suggest a novel link between the genetic regulation of aging and aging-related disease and once again use unique characteristics of *C. elegans*.

In subsequent studies, we and others have demonstrated that the molecular link between these pathways is, in part, maintained by factors that detect and respond to misfolded proteins, heat shock transcription factor (HSF) and molecular chaperones/heat shock proteins. For example, it has been shown that inhibition of HSF-1 function leads to decreased lifespan and an accelerated aging phenotype in *C. elegans* (Garigan *et al.*, 2002; Hsu *et al.*, 2003; Morley and Morimoto, 2004). Conversely, overexpression of HSF-1 in *C. elegans* extends lifespan (Hsu *et al.*, 2003; Morley and Morimoto, 2004). Research on the molecular mechanisms in both areas, aging and molecular chaperones, is active and continuously identifies new players in these pathways. Future work using *C. elegans* will take advantage of new mutants generated from ongoing research to apply the approaches described here.

In addition to our targeted approach to specific genetic pathways for their role as potential modifiers, we used an unbiased genome-wide RNAi screen to identify a set of proteins and pathways that influence polyglutamine aggregation. The identification of five classes of polyglutamine suppressors provides a better understanding of the breadth of pathways and cellular complexes involved in sensing protein damage. In particular, our findings suggest a model in which each step in the birth, life, and death of a protein influences the capacity of a cell to maintain the conditions necessary for protein folding. For example, we found that perturbation of the RNA-processing machinery was associated with accelerated aggregation of Q35::YFP. Although a direct effect is possible, it seems more likely that this results from an increased burden of abnormal proteins requiring the activity of the protein folding buffer. Under such conditions, aggregation-prone proteins normally degraded escape quality control, leading to aggregation and toxicity. Uncovering the role of these genes in the disease process additionally provides new potential therapeutic targets.

Together, these studies have revealed a common set of factors that link the genetic regulation of protein homeostasis, stress responsiveness, and longevity. Using *C. elegans* as a model system, we have combined a variety of approaches, including RNAi, genetics, and behavioral assays with the visualization of polyglutamine proteins in a live, aging, multicellular model to examine polyglutamine pathogenesis. Extending the visualization of polyglutamine proteins to include FRAP and FRET has made it possible to apply quantitative criteria of solubility and intermolecular interactions to visible changes in protein localization and further our understanding of polyglutamine pathogenesis in a highly sensitive, cell-specific manner. In the future, the continued application of this combination of approaches will provide additional insight on the mechanisms underlying protein aggregation and how it contributes to pathology in human disease.

Acknowledgments

We thank members of the Morimoto laboratory past and present, who contributed to this work both intellectually and technically. H. R. B. was supported by the Cellular and Molecular Biology of Disease Training Grant T32 GM08061 from the National Institute of General Medical Sciences (NIGMS) to Northwestern University. J. F. M. was supported by a Medical Scientist Training Grant from NIGMS to Northwestern University and an individual NRSA from the National Institute of Neurological Disease and Stroke. S. M. G. was supported by a PhD fellowship Praxis XXI BD/21451/99 from Fundação para a Ciência e Tecnologia. These studies were also supported by grants from NIGMS (GM38109), the National Institutes of Aging, the Huntington Disease Society of America Coalition for the Cure, and the Daniel F. and Ada L. Rice Foundation.

References

Andrew, S. E., Goldberg, Y. P., Kremer, B., Telenius, H., Theilmann, J., Adam, S., Starr, E., Squitieri, F., Lin, B., Kalchman, M. A., Graham, R. K., and Hayden, M. (1993). The relationship between trinucleotide (CAG) repeat length and clinical features of Huntington's disease. *Nat. Genet.* **4,** 398–403.

Ashrafi, K., Chang, F. Y., Watts, J. L., Fraser, A. G., Kamath, R. S., Ahringer, J., and Ruvkun, G. (2003). Genome-wide RNAi analysis of *Caenorhabditis elegans* fat regulatory genes. *Nature* **421,** 268–272.

Berney, C., and Danuser, G. (2003). FRET or no FRET: A quantitative comparison. *Biophys. J.* **84,** 3992–4010.

Bonini, N. M. (2002). Chaperoning brain degeneration. *Proc. Natl. Acad. Sci. USA* **99**(Suppl. 4), 16407–16411.

Brenner, S. (1974). The genetics of *Caenorhabditis elegans*. *Genetics* **77,** 71–94.

Brinkman, R. R., Mezei, M. M., Theilmann, J., Almqvist, E., and Hayden, M. R. (1997). The likelihood of being affected with Huntington disease by a particular age, for a specific CAG size. *Am. J. Hum. Genet.* **60,** 1202–1210.

Carmichael, J., Chatellier, J., Woolfson, A., Milstein, C., Fersht, A. R., and Rubinsztein, D. C. (2000). Bacterial and yeast chaperones reduce both aggregate formation and cell death in mammalian cell models of Huntington's disease. *Proc. Natl. Acad. Sci. USA* **97,** 9701–9705.

Chai, Y., Koppenhafer, S. L., Bonini, N. M., and Paulson, H. L. (1999). Analysis of the role of heat shock protein (Hsp) molecular chaperones in polyglutamine disease. *J. Neurosci.* **19,** 10338–10347.

Chai, Y., Wu, L., Griffin, J. D., and Paulson, H. L. (2001). The role of protein composition in specifying nuclear inclusion formation in polyglutamine disease. *J. Biol. Chem.* **276,** 44889–44897.

Chan, H. Y., Warrick, J. M., Andriola, I., Merry, D., and Bonini, N. M. (2002). Genetic modulation of polyglutamine toxicity by protein conjugation pathways in *Drosophila*. *Hum. Mol. Genet.* **11,** 2895–2904.

Chen, H. K., Fernandez-Funez, P., Acevedo, S. F., Lam, Y. C., Kaytor, M. D., Fernandez, M. H., Aitken, A., Skoulakis, E. M., Orr, H. T., Botas, J., and Zoghbi, H. Y. (2003). Interaction of Akt-phosphorylated ataxin-1 with 14-3-3 mediates neurodegeneration in spinocerebellar ataxia type 1. *Cell* **113,** 457–468.

Chen, S., Berthelier, V., Yang, W., and Wetzel, R. (2001). Polyglutamine aggregation behavior *in vitro* supports a recruitment mechanism of cytotoxicity. *J. Mol. Biol.* **311,** 173–182.

Chen, S., Ferrone, F. A., and Wetzel, R. (2002). Huntington's disease age-of-onset linked to polyglutamine aggregation nucleation. *Proc. Natl. Acad. Sci. USA* **99,** 11884–11889.

Cummings, C. J., Mancini, M. A., Antalffy, B., DeFranco, D. B., Orr, H. T., and Zoghbi, H. Y. (1998). Chaperone suppression of aggregation and altered subcellular proteasome localization imply protein misfolding in SCA1. *Nat. Genet.* **19,** 148–154.

Cummings, C. J., Sun, Y., Opal, P., Antalffy, B., Mestril, R., Orr, H. T., Dillmann, W. H., and Zoghbi, H. Y. (2001). Over-expression of inducible HSP70 chaperone suppresses neuropathology and improves motor function in SCA1 mice. *Hum. Mol. Genet.* **10,** 1511–1518.

Davies, S. W., Turmaine, M., Cozens, B. A., DiFiglia, M., Sharp, A. H., Ross, C. A., Scherzinger, E., Wanker, E. E., Mangiarini, L., and Bates, G. P. (1997). Formation of neuronal intranuclear inclusions underlies the neurological dysfunction in mice transgenic for the HD mutation. *Cell* **90,** 537–548.

Dobson, C. M. (2001). Protein folding and its links with human disease. *Biochem. Soc. Symp.* **68,** 1–26.

Driscoll, M., and Gerstbrein, B. (2003). Dying for a cause: Invertebrate genetics takes on human neurodegeneration. *Nat. Rev. Genet.* **4,** 181–194.

Faber, P. W., Alter, J. R., MacDonald, M. E., and Hart, A. C. (1999). Polyglutamine-mediated dysfunction and apoptotic death of a *Caenorhabditis elegans* sensory neuron. *Proc. Natl. Acad. Sci. USA* **96,** 179–184.

Faber, P. W., Voisine, C., King, D. C., Bates, E. A., and Hart, A. C. (2002). Glutamine/proline-rich PQE-1 proteins protect *Caenorhabditis elegans* neurons from huntingtin polyglutamine neurotoxicity. *Proc. Natl. Acad. Sci. USA* **99,** 17131–17136.

Feany, M. B., and Bender, W. W. (2000). A Drosophila model of Parkinson's disease. *Nature* **404,** 394–398.

Fernandez-Funez, P., Nino-Rosales, M. L., de Gouyon, B., She, W. C., Luchak, J. M., Martinez, P., Turiegano, E., Benito, J., Capovilla, M., Skinner, P. J., McCall, A., Canal, I., Orr, H. T., Zoghbi, H. Y., and Botas, J. (2000). Identification of genes that modify ataxin-1-induced neurodegeneration. *Nature* **408,** 101–106.

Fire, A., Xu, S., Montgomery, M. K., Kostas, S. A., Driver, S. E., and Mello, C. C. (1998). Potent and specific genetic interference by double-stranded RNA in *Caenorhabditis elegans*. *Nature* **391,** 806–811.

Fraser, A. G., Kamath, R. S., Zipperlen, P., Martinez-Campos, M., Sohrmann, M., and Ahringer, J. (2000). Functional genomic analysis of *C. elegans* chromosome I by systematic RNA interference. *Nature* **408,** 325–330.

Garigan, D., Hsu, A. L., Fraser, A. G., Kamath, R. S., Ahringer, J., and Kenyon, C. (2002). Genetic analysis of tissue aging in *Caenorhabditis elegans*: A role for heat-shock factor and bacterial proliferation. *Genetics* **161,** 1101–1112.

Guarente, L., and Kenyon, C. (2000). Genetic pathways that regulate ageing in model organisms. *Nature* **408,** 255–262.

Hsu, A. L., Murphy, C. T., and Kenyon, C. (2003). Regulation of aging and age-related disease by DAF-16 and heat-shock factor. *Science* **300,** 1142–1145.

Kakizuka, A. (1998). Protein precipitation: A common etiology in neurodegenerative disorders? *Trends Genet.* **14,** 396–402.

Kamath, R. S., Fraser, A. G., Dong, Y., Poulin, G., Durbin, R., Gotta, M., Kanapin, A., Le Bot, N., Moreno, S., Sohrmann, M., Welchman, D. P., Zipperlen, P., and Ahringer, J. (2003). Systematic functional analysis of the *Caenorhabditis elegans* genome using RNAi. *Nature* **421,** 231–237.

Kamino, K., Orr, H. T., Payami, H., Wijsman, E. M., Alonso, M. E., Pulst, S. M., Anderson, L., O'Dahl, S., Nemens, E., White, E., *et al*. (1992). Linkage and mutational analysis of familial Alzheimer disease kindreds for the APP gene region. *Am. J. Hum. Genet.* **51,** 998–1014.

Kawaguchi, Y., Okamoto, T., Taniwaki, M., Aizawa, M., Inoue, M., Katayama, S., Kawakami, H., Nakamura, S., Nishimura, M., Akiguchi, M., Kimura, J., Narumiya, S., and Kakizuka, A. (1994). CAG expansions in a novel gene for Machado–Joseph disease at chromosome 14q32.1. *Nat. Genet.* **8,** 221–228.

Kayed, R., Head, E., Thompson, J. L., McIntire, T. M., Milton, S. C., Cotman, C. W., and Glabe, C. G. (2003). Common structure of soluble amyloid oligomers implies common mechanism of pathogenesis. *Science* **300,** 486–489.

Kim, S., Nollen, E. A., Kitagawa, K., Bindokas, V. P., and Morimoto, R. I. (2002). Polyglutamine protein aggregates are dynamic. *Nat. Cell. Biol.* **4,** 826–831.

Koide, R., Ikeuchi, T., Onodera, O., Tanaka, H., Igarashi, S., Endo, K., Takahashi, H., Kondo, R., Ishikawa, A., Hayashi, A., Saito, M., Tomoda, A., Miike, T., Naito, H., Ikuta, F., and Tsuji, S. (1994). Unstable expansion of CAG repeat in hereditary dentatorubral-pallidoluysian atrophy (DRPLA). *Nat. Genet.* **6,** 9–13.

Kopito, R. R., and Ron, D. (2000). Conformational disease. *Nat. Cell Biol.* **2,** E207–E209.

La Spada, A. R., Wilson, E. M., Lubahn, D. B., Harding, A. E., and Fischbeck, K. H. (1991). Androgen receptor gene mutations in X-linked spinal and bulbar muscular atrophy. *Nature* **352,** 77–79.

Laing, N. G., and Siddique, T. (1997). Cu/Zn superoxide dismutase gene mutations in amyotrophic lateral sclerosis: Correlation between genotype and clinical features. *J. Neurol. Neurosurg. Psychiatry* **63,** 815.

Lee, V. M., Kenyon, T. K., and Trojanowski, J. Q. (2005). Transgenic animal models of tauopathies. *Biochim. Biophys. Acta* **1739,** 251–259.

Lin, K., Dorman, J. B., Rodan, A., and Kenyon, C. (1997). daf-16: An HNF-3/forkhead family member that can function to double the life-span of *Caenorhabditis elegans*. *Science* **278,** 1319–1322.

Link, C. D. (1995). Expression of human beta-amyloid peptide in transgenic *Caenorhabditis elegans*. *Proc. Natl. Acad. Sci. USA* **92,** 9368–9372.

Link, C. D. (2001). Transgenic invertebrate models of age-associated neurodegenerative diseases. *Mech. Ageing Dev.* **122,** 1639–1649.

Lucking, C. B., Durr, A., Bonifati, V., Vaughan, J., De Michele, G., Gasser, T., Harhangi, B. S., Meco, G., Denefle, P., Wood, N. W., Agid, Y., and Brice, A. (2000). Association between early-onset Parkinson's disease and mutations in the parkin gene. French Parkinson's Disease Genetics Study Group. *N. Engl. J. Med.* **342,** 1560–1567.

Mangiarini, L., Sathasivam, K., Seller, M., Cozens, B., Harper, A., Hetherington, C., Lawton, M., Trottier, Y., Lehrach, H., Davies, S. W., and Bates, G. P. (1996). Exon 1 of the HD gene with an expanded CAG repeat is sufficient to cause a progressive neurological phenotype in transgenic mice. *Cell* **87,** 493–506.

Mello, C. C., Kramer, J. M., Stinchcomb, D., and Ambros, V. (1991). Efficient gene transfer in *C. elegans*: Extrachromosomal maintenance and integration of transforming sequences. *EMBO J.* **10,** 3959–3970.

Miyawaki, A. (2003). Visualization of the spatial and temporal dynamics of intracellular signaling. *Dev. Cell* **4,** 295–305.

Miyawaki, A., and Tsien, R. Y. (2000). Monitoring protein conformations and interactions by fluorescence resonance energy transfer between mutants of green fluorescent protein. *Methods Enzymol.* **327,** 472–500.

Mizuno, Y., Hattori, N., Kitada, T., Matsumine, H., Mori, H., Shimura, H., Kubo, S., Kobayashi, H., Asakawa, S., Minoshima, S., and Shimizu, N. (2001). Familial Parkinson's disease. Alpha-synuclein and parkin. *Adv. Neurol.* **86,** 13–21.

Morley, J. F., Brignull, H. R., Weyers, J. J., and Morimoto, R. I. (2002). The threshold for polyglutamine-expansion protein aggregation and cellular toxicity is dynamic and influenced by aging in *Caenorhabditis elegans*. *Proc. Natl. Acad. Sci. USA* **99,** 10417–10422.

Morley, J. F., and Morimoto, R. I. (2004). Regulation of longevity in *Caenorhabditis elegans* by heat shock factor and molecular chaperones. *Mol. Biol. Cell* **15,** 657–664.

Morris, J. Z., Tissenbaum, H. A., and Ruvkun, G. (1996). A phosphatidylinositol-3-OH kinase family member regulating longevity and diapause in *Caenorhabditis elegans*. *Nature* **382,** 536–539.

Nollen, E. A., Garcia, S. M., van Haaften, G., Kim, S., Chavez, A., Morimoto, R. I., and Plasterk, R. H. (2004). Genome-wide RNA interference screen identifies previously undescribed regulators of polyglutamine aggregation. *Proc. Natl. Acad. Sci. USA* **101,** 6403–6408.

O'Nuallain, B., and Wetzel, R. (2002). Conformational Abs recognizing a generic amyloid fibril epitope. *Proc. Natl. Acad. Sci. USA* **99,** 1485–1490.

Oeda, T., Shimohama, S., Kitagawa, N., Kohno, R., Imura, T., Shibasaki, H., and Ishii, N. (2001). Oxidative stress causes abnormal accumulation of familial amyotrophic lateral sclerosis-related mutant SOD1 in transgenic *Caenorhabditis elegans*. *Hum. Mol. Genet.* **10,** 2013–2023.

Ogg, S., Paradis, S., Gottlieb, S., Patterson, G. I., Lee, L., Tissenbaum, H. A., and Ruvkun, G. (1997). The Fork head transcription factor DAF-16 transduces insulin-like metabolic and longevity signals in *C. elegans*. *Nature* **389,** 994–999.

Ordway, J. M., Tallaksen-Greene, S., Gutekunst, C. A., Bernstein, E. M., Cearley, J. A., Wiener, H. W., Dure, L. S.t., Lindsey, R., Hersch, S. M., Jope, R. S., Albin, R. L., and Detloff, P. J. (1997). Ectopically expressed CAG repeats cause intranuclear inclusions and a progressive late onset neurological phenotype in the mouse. *Cell* **91,** 753–763.

Orr, H. T. (2001). Beyond the Qs in the polyglutamine diseases. *Genes Dev.* **15,** 925–932.

Orr, H. T., Chung, M. Y., Banfi, S., Kwiatkowski, T. J., Jr., Servadio, A., Beaudet, A. L., McCall, A. E., Duvick, L. A., Ranum, L. P., and Zoghbi, H. Y. (1993). Expansion of an unstable trinucleotide CAG repeat in spinocerebellar ataxia type 1. *Nat. Genet.* **4,** 221–226.

Parker, J. A., Connolly, J. B., Wellington, C., Hayden, M., Dausset, J., and Neri, C. (2001). Expanded polyglutamines in *Caenorhabditis elegans* cause axonal abnormalities and severe dysfunction of PLM mechanosensory neurons without cell death. *Proc. Natl. Acad. Sci. USA* **98,** 13318–13323.

Phair, R. D., and Misteli, T. (2000). High mobility of proteins in the mammalian cell nucleus. *Nature* **404,** 604–609.

Polymeropoulos, M. H., Lavedan, C., Leroy, E., Ide, S. E., Dehejia, A., Dutra, A., Pike, B., Root, H., Rubenstein, J., Boyer, R., Stenroos, E. S., Chandrasekharappa, S., Athanassiadou, A., Papapetropoulos, T., Johnson, W. G., Lazzarini, A. M., Duvoisin, R. C., Di Iorio, G., Golbe, L. I., and Nussbaum, R. L. (1997). Mutation in the alpha-synuclein gene identified in families with Parkinson's disease. *Science* **276,** 2045–2047.

Rosen, D. R., Siddique, T., Patterson, D., Figlewicz, D. A., Sapp, P., Hentati, A., Donaldson, D., Goto, J., O'Regan, J. P., Deng, J. P., *et al.* (1993). Mutations in Cu/Zn superoxide dismutase gene are associated with familial amyotrophic lateral sclerosis. *Nature* **362,** 59–62.

Ross, C. A. (2002). Polyglutamine pathogenesis: Emergence of unifying mechanisms for Huntington's disease and related disorders. *Neuron* **35,** 819–822.

Satyal, S. H., Schmidt, E., Kitagawa, K., Sondheimer, N., Lindquist, S., Kramer, J. M., and Morimoto, R. I. (2000). Polyglutamine aggregates alter protein folding homeostasis in *Caenorhabditis elegans*. *Proc. Natl. Acad. Sci. USA* **97,** 5750–5755.

Scherzinger, E., Lurz, R., Turmaine, M., Mangiarini, L., Hollenbach, B., Hasenbank, R., Bates, G. P., Davies, S. W., Lehrach, H., and Wanker, E. E. (1997). Huntingtin-encoded

polyglutamine expansions form amyloid-like protein aggregates *in vitro* and *in vivo*. *Cell* **90,** 549–558.

Shulman, J. M., Shulman, L. M., Weiner, W. J., and Feany, M. B. (2003). From fruit fly to bedside: Translating lessons from *Drosophila* models of neurodegenerative disease. *Curr. Opin. Neurol.* **16,** 443–449.

Stefani, M., and Dobson, C. M. (2003). Protein aggregation and aggregate toxicity: New insights into protein folding, misfolding diseases and biological evolution. *J. Mol. Med.* **81,** 678–699.

Thompson, L. M., and Marsh, J. L. (2003). Invertebrate models of neurologic disease: Insights into pathogenesis and therapy. *Curr. Neurol. Neurosci. Rep.* **3,** 442–448.

Trottier, Y., Lutz, Y., Stevanin, G., Imbert, G., Devys, D., Cancel, G., Saudou, F., Weber, C., David, G., Tora, L., Agid, Y., Brice, A., and Mandel, J. L. (1995). Polyglutamine expansion as a pathological epitope in Huntington's disease and four dominant cerebellar ataxias. *Nature* **378,** 403–406.

Tsien, R. Y. (1998). The green fluorescent protein. *Annu. Rev. Biochem.* **67,** 509–544.

Wang, J., and Barr, M. M. (2005). RNA interference in *Caenorhabditis elegans*. *Methods Enzymol.* **392,** 36–55.

Warrick, J. M., Chan, H. Y., Gray-Board, G. L., Chai, Y., Paulson, H. L., and Bonini, N. M. (1999). Suppression of polyglutamine-mediated neurodegeneration in *Drosophila* by the molecular chaperone HSP70. *Nat. Genet.* **23,** 425–428.

Warrick, J. M., Paulson, H. L., Gray-Board, G. L., Bui, Q. T., Fischbeck, K. H., Pittman, R. N., and Bonini, N. M. (1998). Expanded polyglutamine protein forms nuclear inclusions and causes neural degeneration in *Drosophila*. *Cell* **93,** 939–949.

Westlund, B., Stilwell, G., and Sluder, A. (2004). Invertebrate disease models in neurotherapeutic discovery. *Curr. Opin. Drug Discov. Dev.* **7,** 169–178.

Wexler, N. S., Lorimer, J., Porter, J., Gomez, F., Moskowitz, C., Shackell, E., Marder, K., Penchaszadeh, G., Roberts, S. A., Gayan, J., Brocklebank, D., Cherny, S. S., Cardon, L. R., Gray, J., Dlouhy, S. R., Wiktorski, S., Hodes, M. E., Conneally, P. M., Penney, J. B., Gusella, J., Cha, J. H., Irizarry, M., Rosas, D., Hersch, S., Hollingsworth, Z., MacDonald, M., Young, A. B., Andresen, J. M., Housman, D. E., De Young, M. M., Bonilla, E., Stillings, T., Negrette, A., Snodgrass, S. R., Martinez-Jaurrieta, M. D., Ramos-Arroyo, M. A., Bickham, J., Ramos, J. S., Marshall, F., Shoulson, I., Rey, G. J., Feigin, A., Arnheim, N., Acevedo-Cruz, A., Acosta, L., Alvir, J., Fischbeck, K., Thompson, L. M., Young, A., Dure, L., O'Brien, C. J., Paulsen, J., Brickman, A., Krch, D., Peery, S., Hogarth, P., Higgins, D. S., Jr., and Landwehrmeyer, B. (2004). Venezuelan kindreds reveal that genetic and environmental factors modulate Huntington's disease age of onset. *Proc. Natl. Acad. Sci. USA* **101,** 3498–3503.

Wouters, F. S., Bastiaens, P. I., Wirtz, K. W., and Jovin, T. M. (1998). FRET microscopy demonstrates molecular association of non-specific lipid transfer protein (nsL-TP) with fatty acid oxidation enzymes in peroxisomes. *EMBO J.* **17,** 7179–7189.

Zoghbi, H. Y., and Orr, H. T. (2000). Glutamine repeats and neurodegeneration. *Annu. Rev. Neurosci.* **23,** 217–247.